Repetitive mild traumatic brain injury causes neuronal damage in the APP/PS1 mouse model of Alzheimer's disease without an enduring impact on amyloid pathology, sleep, or epileptiform activity

JEFFEREY YUE[a,b]*, VICTORIA CARRIQUIRIBORDE[a,c]*, WAI HANG CHENG[d], TAHA YILDIRIM[c], JIANJIA FAN[d], SEAN TOK[a,c], MICHAEL KELLY[c], CHERYL L. WELLINGTON[d,e,f,g], BRIANNE A. KENT[a,c]

a. Institute for Neuroscience and Neurotechnology, Simon Fraser University, 8888 University Drive, Burnaby, BC, Canada, V5A 1S6
b. Department of Molecular Biology and Biochemistry, Simon Fraser University, 8888 University Drive, Burnaby, BC, Canada, V5A 1S6
c. Department of Psychology, Simon Fraser University, 8888 University Drive, Burnaby, BC, Canada, V5A 1S6
d. Department of Pathology and Laboratory Medicine, University of British Columbia, 2215 Wesbrook Mall, Vancouver, BC, Canada, V6T 1Z3
e. Djavad Mowafaghian Centre for Brain Health, University of British Columbia, 2215 Wesbrook Mall, Vancouver, BC V6T 1Z3
f. School of Biomedical Engineering, University of British Columbia, 2215 Wesbrook Mall, Vancouver, BC V6T 1Z3
g. International Collaboration on Repair Discoveries, Blusson Spinal Cord Centre, Vancouver General Hospital, 818 W 10th Ave, Vancouver, BC V5Z 1N1

*These authors contributed equally

Correspondence:
Brianne A Kent
bkent@sfu.ca
Simon Fraser University
Department of Psychology
8888 University Drive
Burnaby, BC
Canada

Key words

Concussion, Alzheimer's disease, EEG, sleep, seizure, amyloid, transgenic mouse model

Abstract

Traumatic Brain Injury (TBI) is a known risk factor for Alzheimer's disease and related neurodegenerative diseases. Sleep disturbances and epileptiform abnormalities can appear after TBI and may contribute to the development of neuropathology. In this study, we characterized sleep, epileptiform activity, and neuropathology after repetitive mild traumatic brain injury (rmTBI) in a mouse model of Alzheimer's disease. We used the Closed Head Impact Model of Engineered Rotational Acceleration (CHIMERA) to deliver rmTBI or sham (control) treatment to 6-month-old APP/PS1 mice (n=19). One month post-injury, we implanted electroencephalogram (EEG) and electromyographic (EMG) electrodes, recorded for 72 hours, and then collected brain tissue and blood plasma. Our assessment of sleep architecture showed that time spent in vigilance state was not affected by the rmTBI one month post-injury; however, power spectra analysis showed a statistically significant shift towards higher frequencies in the rmTBI group during non-rapid eye movement (NREM) sleep. Epileptiform activity did not differ between sham and rmTBI. Compared to sham controls, the rmTBI group showed higher neurofilament light (NF-L), but not glial-fibrillary acidic protein (GFAP) in blood plasma and no change in amyloid pathology. These results indicate sustained neurological injury in the APP/PS1 mice one month after rmTBI without affecting amyloid deposition in the brain. Our study suggests that rmTBI can induce neural injury without causing enduring sleep disruption, seizures, and exacerbation of amyloidosis in the APP/PS1 mouse model.

Introduction:

Traumatic brain injury (TBI) is a leading cause of global morbidity and mortality and a risk factor for neurodegenerative diseases, such as Alzheimer's disease (Lefevre-Dognin et al., 2021; Van Den Heuvel et al., 2007). TBI severity ranges from mild to severe, with mild TBI (mTBI) accounting for approximately 90% of cases (Maas et al., 2022).

Repetitive TBI, even if each is mild, can lead to enduring symptoms in approximately 20% of patients (Theadom et al., 2020). It is thought that the repetitive mTBI (rmTBI) synergize and have a greater than expected impact on cognitive and executive function (Guskiewicz et al., 2003; Montenigro et al., 2017). rmTBI can cause persistent neurocognitive dysfunction, affecting attention, information processing, and memory, as well as chronic comorbidities, such as post-traumatic stress disorder (PTSD), depression, substance abuse, pain, insomnia, and fatigue (Golden & Zusman, 2019; Howlett et al., 2022; Karr et al., 2014; Sandsmark et al., 2017). Pre-clinical studies using animal models have shown that rmTBI are associated with cognitive impairments, microgliosis, and axonal damage, as well as increased neuronal excitability, all of which are hallmarks of AD pathology (Bugay et al., 2020; Cheng et al., 2019; Moro et al., 2023; Namjoshi et al., 2014). rmTBI in transgenic animal models of AD have also shown exacerbated neuropathology development, including the accumulation of Aβ (Cheng et al., 2018; Conte et al., 2004; Uryu et al., 2002).

In addition to impacting cognition and increasing the risk of neurodegenerative disease, rmTBI can cause sleep disturbances and posttraumatic epilepsy (PTE) (Bugay et al., 2020; Petraglia et al., 2014; Sandsmark et al., 2017; Shandra et al., 2019), both of which are independent risk factors for neurodegenerative disease (Kent et al., 2021; Palop et al., 2007; Vossel et al., 2017). The most prevalent sleep disturbances reported in humans after rmTBI are insomnia and hypersomnia (Aoun et al., 2019; Sandsmark et al., 2017). In mouse models, rmTBI can cause reduced sleep duration,

starting from 3 months post-injury (Morris et al., 2024), as well as sleep fragmentation (Petraglia et al., 2014). Other EEG measures, such as spectral power, which is a quantitative EEG (qEEG) analysis, have also been shown to be affected by rmTBI (Massimini et al., 2024; Modarres et al., 2017; Nwakamma et al., 2024). In humans, PTE can be accompanied by cognitive deficits, sleep disturbances, and mood changes (Konduru et al., 2021; Saletti et al., 2021). The proportion of patients with PTE increases with injury severity (Saletti et al., 2021), yet it is still unclear whether repetitive impacts can increase PTE susceptibility. How the post-rmTBI sleep disturbances or epileptiform activity contribute to the risk or progression of neurodegeneration is not yet clear.

Here, we investigated the effects of rmTBI in APP/PS1 mice (Jankowsky et al., 2001), followed by EEG/EMG recording and quantification of multiple protein targets through immunoassays. As most previous studies have focused either on severe TBI or acute time points post-injury, to our knowledge, this is the first study investigating the mutual effects on sleep impairment, epileptiform activity, and neuropathology as a result of rmTBI in a mouse model of AD one month post-injury. We found that even though there were signs of enduring neuronal damage, there were no changes in sleep architecture, seizure susceptibility, epileptiform activity, or amyloid pathology one month post-injury.

Methods

Animals:

All procedures in this study were approved by the Simon Fraser University Animal Ethics Committee (Protocol 1330P-21) and followed the guidelines from the Canadian Council on Animal Care. Figure 1 illustrates the study protocol. This study adheres to the Animal Research: Reporting of In Vivo Experiments (ARRIVE) guidelines for reporting of animal research.

The mouse strain used for this research project, B6C3-Tg(APPswe,PSEN1dE9)85Dbo/Mmjax, RRID:MMRRC_034829-JAX, was obtained from the Mutant Mouse Resource and Research Center (MMRRC) at The Jackson Laboratory, an NIH-funded strain repository, and was donated to the MMRRC by David Borchelt, Ph.D., McKnight Brain Institute, University of Florida. APP/PS1 mice are double transgenic mice that overexpress mouse/human APP containing the Swedish mutation (K595N/M596/L) and a mutant human presenilin 1 (PS1 delta E9). Both males (n=8) and females (n=11) were used in this study. All 19 animals were single housed in plastic clear cages under a 12:12 LD cycle. Food and water were available *ad libitum*.

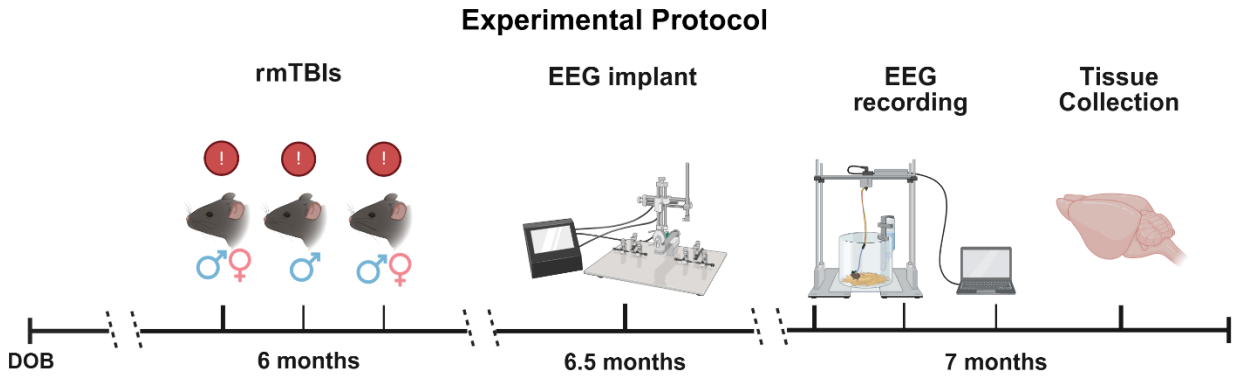

Figure 1. Schematic diagram illustrating the experimental protocol. At six months of age APP/PS1 mice received rmTBI. Male mice received 3 consecutive mTBI 24 h apart, and female mice received two mTBI 48 h apart. After recovering, mice received EEG/EMG intracranial implantation. Two weeks after implantation, at 7 months of age, the mice underwent 72 h of EEG/EMG recording. Tissue collection was completed immediately after recording. Created in BioRender https://BioRender.com/6h4as63

1. Repetitive mild TBI (CHIMERA)

CHIMERA procedures followed the protocol previously described (Cheng et al., 2019; Namjoshi et al., 2014, 2017). APP/PS1 mice at 6 months of age were randomly assigned to sham (n=8) or rmTBI (n=11) groups. Mice received meloxicam subcutaneously (SQ, 1mg/kg) 30min before being restrained on the CHIMERA device. Mice were anesthetized with isoflurane, received saline (SQ, 0.5mL) for hydration, and eye gel was applied. Total duration of isoflurane exposure was 4-8 min. Sham animals underwent the same procedures except for the CHISMERA impact. For the rmTBI group, the intensity of the impact was lowered for females to compensate for lower body weight and to reduce morbidity. Male mice received 3 mTBI (direct impact at 0.7J) 24h apart, and female mice received two mTBI (direct impact at 0.6J) 48h apart. The 0.7J impact energy is the highest energy within the mTBI parameter as previously defined (Namjoshi et al., 2017). After procedures, mice recovered in a warmed cage supplemented with hydrogel and were returned to the housing room two days after the final mTBI.

2. Injury effects: LRR and Grimace

The loss of righting reflex (LRR) was calculated as the time interval from the termination of isoflurane to the successful attempt of righting for each mouse after injury. The Grimace Scale is a two-point scoring system based on defined facial and physical features of the mice as indicators of pain and discomfort (Langford et al., 2010). Grimace score was recorded once every five minutes. The Grimace recovery time was calculated as the time interval between when each mouse righted their body to the time when all grimace scores were at zero.

3. Electrode implantation

2EEG/1EMG headmount (catalog number 8201-SS; Pinnacle Technology, Lawrence, KS, USA) implant surgery was performed as previously reported (Kent et al., 2018, 2019). Mice were anesthetized with isoflurane and given meloxicam intraperitoneally (IP, 5 mg/kg), lidocaine (SQ, 7 mg/kg), and lubricating eye gel. A middle rostral-caudal incision was made to expose the skull surface. Four stainless steel screw electrodes were inserted into the skull at coordinates relative to bregma: AP +/- 3mm, ML +/- 1.5mm. EMG wires were inserted into the nuchal muscle. A two-part epoxy was applied to screws to ensure good electrical contact, and a multimeter was used to test the electrical contact. The headmount was secured with a layer of dental cement (catalog number 525000; A-M Systems, Sequim, WA, USA). Post-operatively, lactated ringer (SQ, 5mg/kg) was provided for hydration, and buprenorphine (0.05mg/kg) was provided for 3 days for pain relief. All mice were allowed to recover for at least 7 days before EEG recordings.

4. EEG recording

EEG/EMG recordings were collected in a tethered system (8200-K1, Pinnacle Technology) using Sirenia® Acquisition software (version 2.2.1). Sample rate was 400Hz, preamp gain was 100dB, and low-pass filter was 40Hz for EEG and 100Hz for EMG. EEG/EMG was recorded for 72h.

5. Assessment of vigilance state

Assessment of vigilance state was performed using the final 24h of the EEG recording. An experimenter blinded to the experimental condition used cluster scoring followed by visual inspection to score each 10s epoch for wake, NREM, and REM states using Sirenia Sleep Pro software (version 3.0.1). Wake state was defined by a low-amplitude EEG, with a dominant frequency higher than 4Hz, typically accompanied by high EMG activity. NREM was defined by high-amplitude EEG and a dominant frequency of less than 4Hz, usually accompanied by low EMG activity. REM was defined by low-amplitude and uniform waveforms with peak frequency at 4-8Hz and occurring following NREM state. The state of each epoch was defined based on the state dominating more than 50% of the epoch. Epochs containing artifacts (i.e., extremely high power) or without clear recordings (i.e., flat line) were excluded from the analyses. A bout was counted when the animal remained in the same vigilance state for 30s (3 epochs) or more. Bout length was calculated as the average time the animal spent across bouts of NREM, REM, or wake respectively.

6. Spectral Power Analysis

Spectral power provides a quantitative measure of how neural activity is distributed across the frequency bands of interest. We calculated power at each frequency and each electrode separately. First, the raw data were pre-processed by splitting the signal into 10s epochs and applying a 2nd order Butterworth filter (0-40Hz). Then, Welch's method was used to transform the filtered data into the frequency domain using a Hamming window of 10s with a 50% overlap. To calculate relative power, absolute power at each frequency was divided by the total power across frequencies (0.5-30Hz). We only included frequencies 0.5-30Hz to avoid distortions caused by the filter cut-off. We used the PLS method to analyze spectral power data. The input data was a matrix wherein rows represented each individual mouse separated by treatment group (TBI vs sham), and the columns represented the average power at each frequency (0.5-30Hz).

7. Epileptiform Activity Analysis

Seizure detection was performed manually using the Sirenia Seizure Pro software (version 3.0.1). Two researchers blinded to the experimental condition, visually inspected the 72h recordings for seizures. Seizures were defined as high amplitude and high frequency events more than 10s in duration. Heat maps and spectral plots were used to identify epochs with high EEG power and high frequency spectra to aid in the seizure detection. Once a seizure was identified, it was marked, and the window size, step size, and power measurements from this reference seizure were used to identify other seizures.

To detect epileptiform activity (EA) events, we used a semi-automated method to score the last 24h of the recording. We used a bandpass filter (0.5-40Hz) to filter out the high-frequency artefacts and visually identified an example of a spike, poly-spike, and spike-wave discharges (SWD) that fulfilled the definition of each category according to the recommendations by Jin et al. (2022). A

spike was defined as a cortical epileptiform spike (wave) that showed more than 2x the baseline voltage mean. Poly-spikes were defined as two or more spikes with the same amplitude criteria as a spike occurring in succession. Lastly, a SWD was defined as surface-negative spikes alternating with surface-positive waves or vice versa at 7-10Hz with durations between 0.5-5s. All EA were visually verified by a researcher blinded to treatment.

8. Biosample collection

Mice were anesthetized using isoflurane and then euthanized by CO_2. Blood samples were collected via cardiac puncture, and the collected blood samples were mixed with 100mg/mL EDTA to prevent coagulation. Blood samples were centrifuged at 1500g for 20min, and supernatant was collected as plasma. Plasma samples were stored at -80˚C until analysis. Following cardiac puncture, mice were transcardially perfused with ice-cold phosphate buffered saline (PBS, pH 7.4), and brain tissue was extracted. One hemibrain was frozen on dry ice then stored at -80˚C, and the other hemibrain was fixed in 4% paraformaldehyde (PFA) for 3 days, which was then cryoprotected in 30% sucrose. The cryopreserved hemibrain was coronally sectioned at 40µm using cryotome (Leica).

Hemibrain lysate was generated in serial extraction as described with modification (Cheng et al., 2018). Frozen hemibrain was ground using a mortar and pestle, while keeping it at a low temperature with liquid nitrogen. Ground tissue was then homogenized (Ultra-Turrax T25) in four volumes of carbonic buffer containing 100mM Na_2CO_3, 50mM NaCl, and 1mM phenylmethanesulfonyl fluoride (pH 11.5), supplemented with mini-cOmplete protease inhibitor cocktail (1 tablet/10 ml; Roche, cat. # 11836170001) for 20s, then sonicated in 20% output for 10s. The samples were then centrifuged at 16000 g for 45min. The supernatant was collected and neutralized in 1.5 times the volume of 1M Tris-HCl buffer (pH 6.8) to yield a final pH of ~7.4. The pellet was resuspended in four volumes of 5M guanidine hydrochloride (5M GuHCl, 50 mM Tris-HCl, pH 8.0) and incubated at room temperature with rotation for 3h. Both fractions were stored at -80˚C until analysis.

9. Plasma Biomarker Analysis

Plasma levels of murine GFAP were quantified by a customized immunoassay using a pair of rabbit antibodies against mouse GFAP (Abcam, cat # ab244094) with the MesoScale Discovery (MSD) platform as previously published (Button et al., 2021). Plasma was diluted 4 times with PBS containing 1% bovine serum albumin (Sigma Aldrich, cat. # A7906). Plasma levels of murine Nf-L were measured by the MSD Neurofilament-light assay kit (Mesoscale, cat. # K1517XR-2) following the manufacturer's instructions. Murine plasma was diluted 6 times with MSD Diluent 12 for the Nf-L assay. The researcher conducting biomarker analysis was blinded to the experimental conditions. All samples with reported comparisons were analyzed within the same run.

10. Immunohistochemistry

Immunohistochemistry of amyloid plaques was performed with the regions of interest (ROI) defined according to anatomical landmarks illustrated on the Allen mouse brain atlas (https://mouse.brain-map.org/static/atlas). The ROIs include parietal isocortex (ISOCTX) and hippocampus (HPF). The parietal cortex was further divided into retrosplenial cortex (RSP), motor sensory cortex (MS), entorhinal cortex (ENT), and piriform area (PIR) for regional analysis.

Anterior cortical regions investigated include the anterior cingulate area (ACA), frontal motor sensory cortex (F-MS), and frontal piriform area (F-PIR).

Every tenth coronal brain sections at 40 µm-thickness were sampled, and up to three sections per region were analyzed. The sections were washed in 0.05% Triton X-100 diluted in TBS (TBS-T), then incubated serially in 88% formic acid for 5 min, 0.3% hydrogen peroxide diluted in 0.25% Triton X-100, and 5% milk. Sections were then incubated with primary antibody (6E10: 1:1000, BioLegend cat. # 803004) overnight at 4˚C with rocking motion. After washing in TBS-T, sections were incubated in biotinylated secondary antibody (1:1000, Southern Biotech, cat. # 1071-08) for 90 min in room temperature. After washing, the sections were developed with ABC reagent (1:400, Vector Laboratory, cat. # PK-6100), then stained in 0.2 mg/ml 3,3'-Diaminobenzidine (DAB). The sections were mounted onto SuperFrost microscope slides (FisherScientific. cat # 12-550-15) and coverslipped with DPX mounting medium (Sigma Aldrich cat. # 06522). The sections were imaged using an Axio Scan.Z1 slide scanner (Zeiss) at 20x magnification, followed by resizing at 30% and image optimization using the Zen software (version 3.7).

11. $A\beta_{42}$ ELISA

Soluble (carbonic fraction) and insoluble (GuHCl fraction) $A\beta_{42}$ in hemibrain lysates were quantified using a commercial ELISA kit (WAKO, cat # 296-64401) according to the manufacturer's protocol. The carbonic fraction was diluted in 1:100-500 and the GuHCl fraction was diluted in 1:1000-5000. Every sample was loaded in triplicate, and the average value of the three readings was reported.

12. Statistical Analysis

The Shapiro-Wilk test was used to assess data normality (Mishra et al., 2019). For LRR and Grimace scores, data were analyzed using repeated measures two-way ANOVA, followed by post hoc t-tests using the Šídák's correction when appropriate. Male and female mice were analyzed separately.

Graphs and statistical analyses for the vigilance state data were performed using GraphPad (version 10.0.3) and RStudio (version 2024.04.1+748). Mann-Whitney was used to compare rmTBI and sham groups for duration, transition counts, bout counts, bout lengths, and lights on and off states for each vigilance state separately (NREM, REM, wake). Due to the small sample size, sex differences were not tested in our main analysis. However, we conducted a post-hoc test using Kruskal-Wallis with Dunn's correction for multiple comparisons to analyze sex differences. Normalized EEG spectral power data were analyzed using mean-centered partial least squares (PLS) analysis (McIntosh & Lobaugh, 2004) in Matlab (MathWorks R2023a, version 9.14). PLS is a multivariate method adapted for neuroimaging data where dependent measures (e.g., power spectra frequencies) are highly correlated. We used PLS because it allowed us to detect the effects of rmTBI across the whole EEG frequency spectrum in a single analytical step, avoiding the need for multiple comparisons (Cragg et al., 2011). The data structure and analysis steps were similar to those used in Cragg et al. (2011) for power spectra analysis. Through this analysis, we obtained latent variables (LV) for each EEG channel (frontal and parietal) in each vigilance state, corresponding to the contrast and the pattern across frequencies. Statistical significance was established using permutation testing and bootstrap resampling for each LV.

All graphs and statistical analyses of epileptiform activity data were performed using GraphPad (version 10.0.3). Statistical significance for the non-parametric data was tested by Mann-Whitney to compare single spike, poly spikes, and SWD counts between rmTBI and sham groups. Total epileptiform activity across vigilance states was analyzed using Mann-Whitney multiple comparisons with Holm-Šídák correction. Sex differences in epileptiform activity were assessed post-hoc using Kruskal-Wallis with Dunn's correction for multiple comparisons.

Effects of rmTBI on plasma levels of Nf-L and GFAP were analyzed using Mann-Whitney with the assumption that sex does not affect baseline level of both plasma biomarkers. Amyloid histopathology was quantified using ImageJ by measuring the percentage of immunoreactive area within the defined ROIs. Statistical analyses of amyloid histopathology and $A\beta_{42}$ ELISA assay were performed by analyzing main effects (injury vs sex) using two-way ANOVA on GraphPad.

Statistical significance was set at $p \leq 0.05$ for all analyses.

Results

rmTBI induced prolonged recovery

We first characterized injury responses by recording the latency of LRR and Grimace recovery after each mTBI. LRR is used in preclinical TBI studies as a proxy for loss of consciousness in humans, since LRR is associated with memory impairments and neurological abnormalities (Berman et al., 2023). Both sham and TBI mice experienced a similar duration of LRR (Fig. 2A). There was a main effect of injury on grimace recovery time in females (p=0.0099, F (1,9)=10.62) with longer delay in grimace recovery observed in the TBI group compared to the sham controls (Fig. 2B). However, there were no significant differences in the male group (p>0.05). No mice were withdrawn from the study due to morbidity or mortality. These data indicate that the TBI energy delivered to mice aligns within the mild intensity as previously reported (Namjoshi et al., 2017).

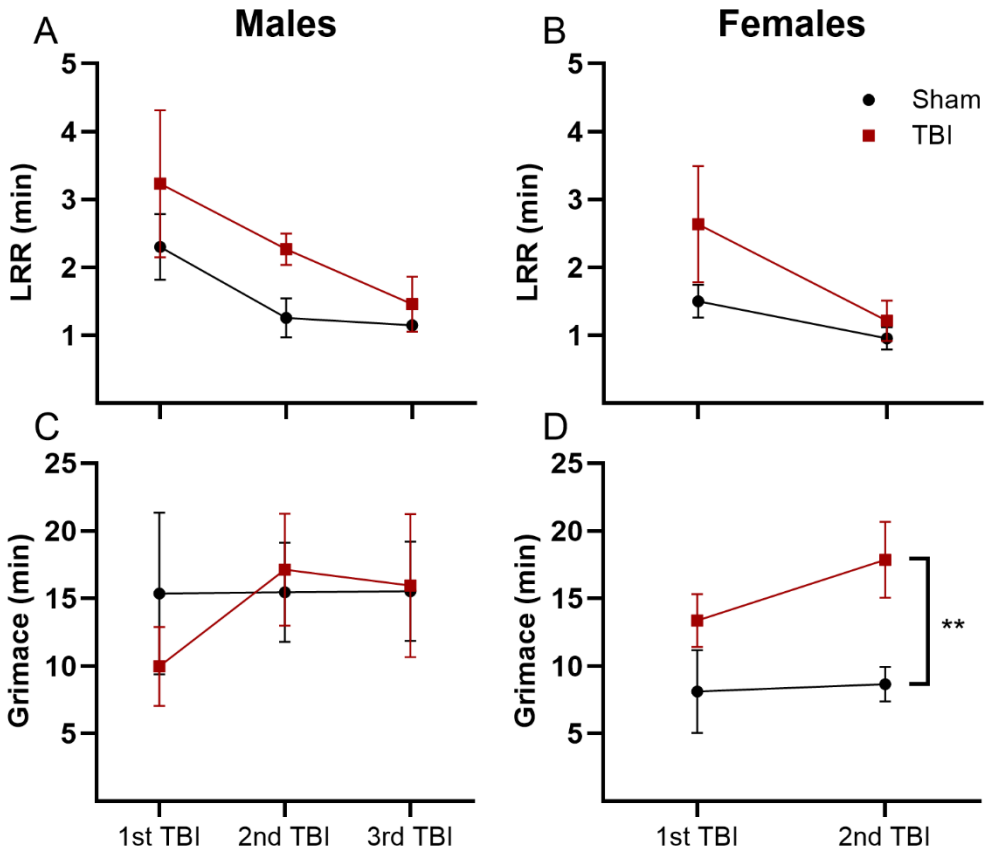

Figure 2. Neurological behaviour after rmTBI. Average LRR duration in minutes for each cohort after each injury timepoint for **(A)** males and **(B)** females. Average amount of time it took to reach a score of zero in the grimace scale in minutes after each injury for **(C)** males and **(D)** females. Results were reported as mean ± SEM and analyzed by repeated measures two-way ANOVA. Sham data is shown in black and rmTBI data is shown in red. Male TBI n=5, male sham n=3; female TBI n=6, females sham n=5. ** p< 0.01.

Sleep architecture did not differ between the rmTBI and sham groups one month post-injury

One female TBI mouse was excluded from all EEG analysis due to poor data quality (i.e., flat line, signal clipping, artifacts). Therefore, only 10 females (n=5 rmTBI, n=5 sham) were used for the EEG analysis. The percentage of time spent in NREM, REM, and wake was similar across the two groups. A Mann-Whitney test revealed no statistically significant difference between the rmTBI and sham groups for the vigilance states (p>0.05; Fig 3A). To evaluate the effects of rmTBI on sleep fragmentation, we assessed transition counts, bout counts, and bout lengths. There were no statistically significant differences between the rmTBI and sham groups in transitions between NREM-REM, NREM-wake, REM-NREM, REM-wake, wake-NREM states (p>0.05; Fig 3B). Bout counts for NREM, REM, and wake states (p>0.05), and bout lengths for NREM, REM, and wake (p>0.05) were not significantly different between the rmTBI and sham groups (Fig 3C). Sex

effects for time spent on each vigilance state, transitions, bout counts, and bout length were analyzed separately with a post-hoc test. No statistically significant difference was found between males and females for either of the measures (p>0.05). Additionally, to evaluate circadian rhythm changes after rmTBI, we analyzed the vigilance states separately during the 12h light phase and 12h dark phase. There were no significant differences between the TBI and sham groups in either of the states (NREM, REM, wake) during the light or dark phases (p>0.05; Supplementary Fig. S1).

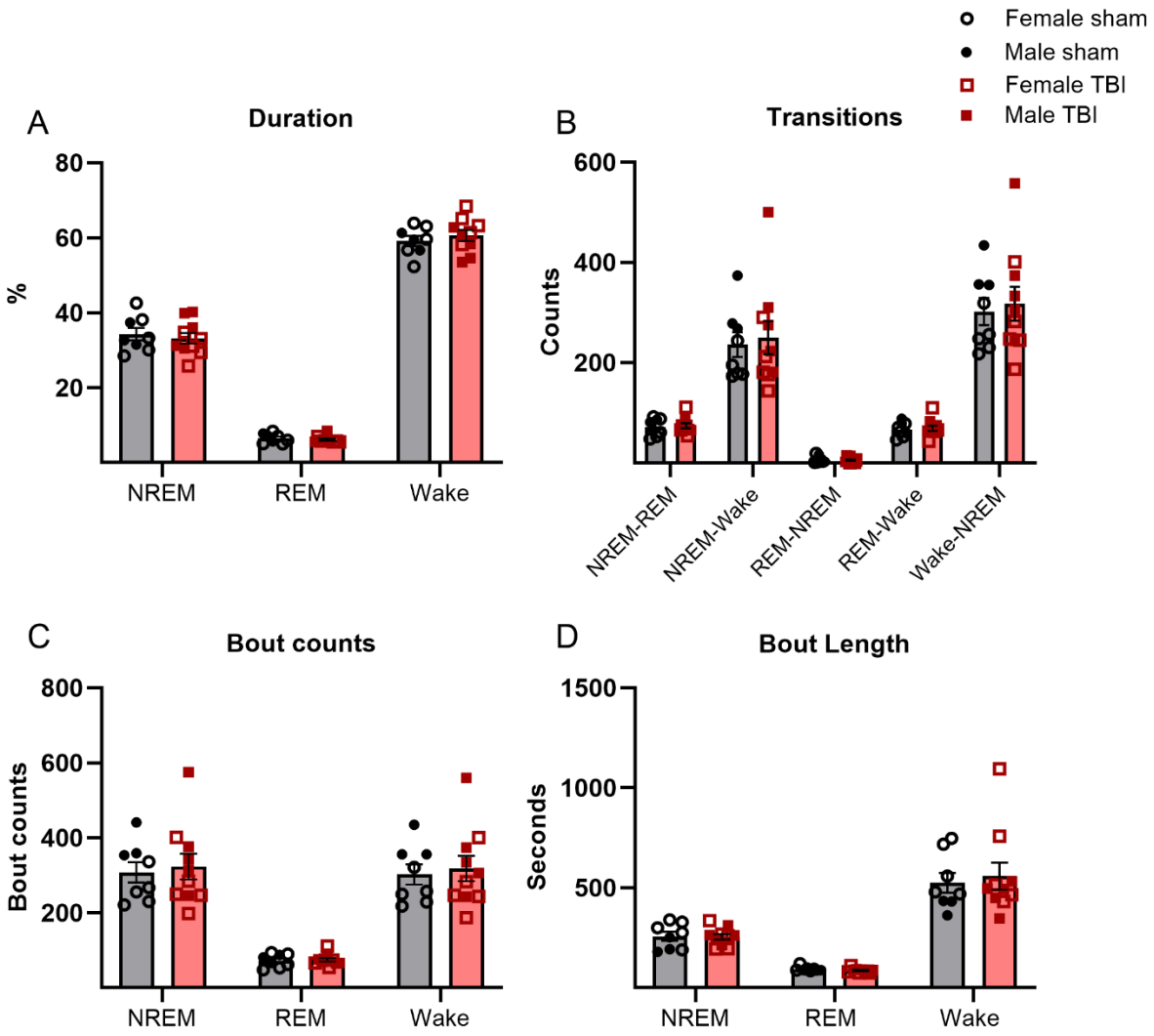

Figure 3. Sleep architecture one month after rmTBI in APP/PS1 mice. (A) Percentage of time spent in NREM, REM, and wake. **(B)** Transition counts between vigilance states NREM-REM, NREM-Wake, REM-NREM, REM-Wake, Wake-NREM. **(C)** Number of 30 s bouts of NREM, REM, and wake. **(D)** Average bout length. All data are expressed in mean ±SEM and analyzed by Mann Whitney-U test. Sham data are shown in black and rmTBI data are down in red. Females are shown with open symbols and males are shown with solid symbols. Each dot represents the average for a single mouse. Male TBI n=5, male sham n=3; female TBI n=5, female sham n=5.

RmTBI causes spectral power shifts during NREM sleep

The PLS analysis identified a significant LV (p=0.041), indicating a difference between the TBI and sham groups during NREM. The TBI group exhibited higher relative power compared to the sham group at the parietal electrode at 5 Hz (theta band) during NREM (Fig. 4). Additionally, the TBI group exhibited higher relative power compared to the sham group across the higher frequencies (11-18 Hz) at the same electrode during NREM (Fig. 4). There was a similar trend at the frontal electrode during NREM, but it was not statistically significant (p>0.05; Supplementary Fig. S2 D). There were no differences observed between the TBI and sham groups during REM at either of the electrode locations (p>0.05; Supplementary Fig. S2 B & E). The spectral graphs during wake show some differences between the TBI and sham group (Supplementary Fig. S2 C & F) in the lower (4-6 Hz) and higher frequencies (20-24 Hz), but none of these were statistically significant (Parietal EEG: p>0.05; Frontal EEG: p>0.05).

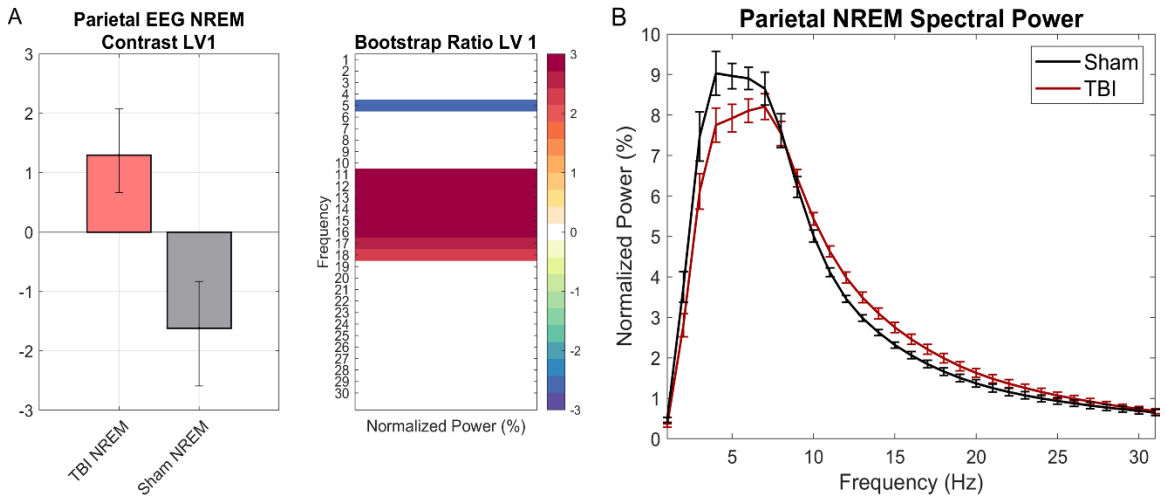

Figure 4. PLS analysis of the spectral power during NREM at the parietal EEG after rmTBI. (A) The PLS contrast in TBI and sham groups during NREM. Error bars represent the 95% confidence interval. The heat map represents the bootstrap ratio of the normalized power for each frequency. Red colors denote higher power in the TBI group whereas blue colors denote higher power in the sham group. Frequencies highlighted by these colors show statistical significance. **(B)** Spectral power with frequencies 0.5-30Hz in the x-axis and the normalized power values in the y-axis. Error bars represent the ±SEM. Sham data is shown in black and the rmTBI data is shown in red. Male TBI n=5, male sham n=3; female TBI n=5, female sham n=5.

Epileptiform activity is not increased by rmTBI one month post-injury

Only one mouse exhibited spontaneous seizures (male, sham). Mann-Whitney revealed no statistical significance in Single Spike (SS), poly spikes (PS), or spike-wake discharges (SWD) counts per hour between the rmTBI and sham groups (p>0.05; Fig. 5A-C).

Additionally, we compared the prevalence of epileptiform activity during the three vigilance states and found no significant differences between the groups (Fig. 5D). However, as observed in previous studies (Gureviciene et al., 2019; Tok, Crauwels, et al., 2022), there was a trend towards an increase in epileptiform activity (EA) prevalence during the sleep states (NREM and REM).

Due to the small sample size, we did not include a statistical analysis of sex differences in our main analysis. However, SWDs were only observed in female mice in both groups. A post-hoc test showed that the difference in SWDs counts between males and females was statistically significant within the rmTBI group (p=0.016; Supplementary Fig. S3) but not the sham group (p=0.065). The post-hoc test also showed that females had statistically significantly more EA per hour than males in the rmTBI group, but only during wake (p=0.025). The other two states, NREM and REM, had no significant sex differences for total EA per hour (p>0.05). There were no sex differences in singles spike or poly spikes counts (p>0.05).

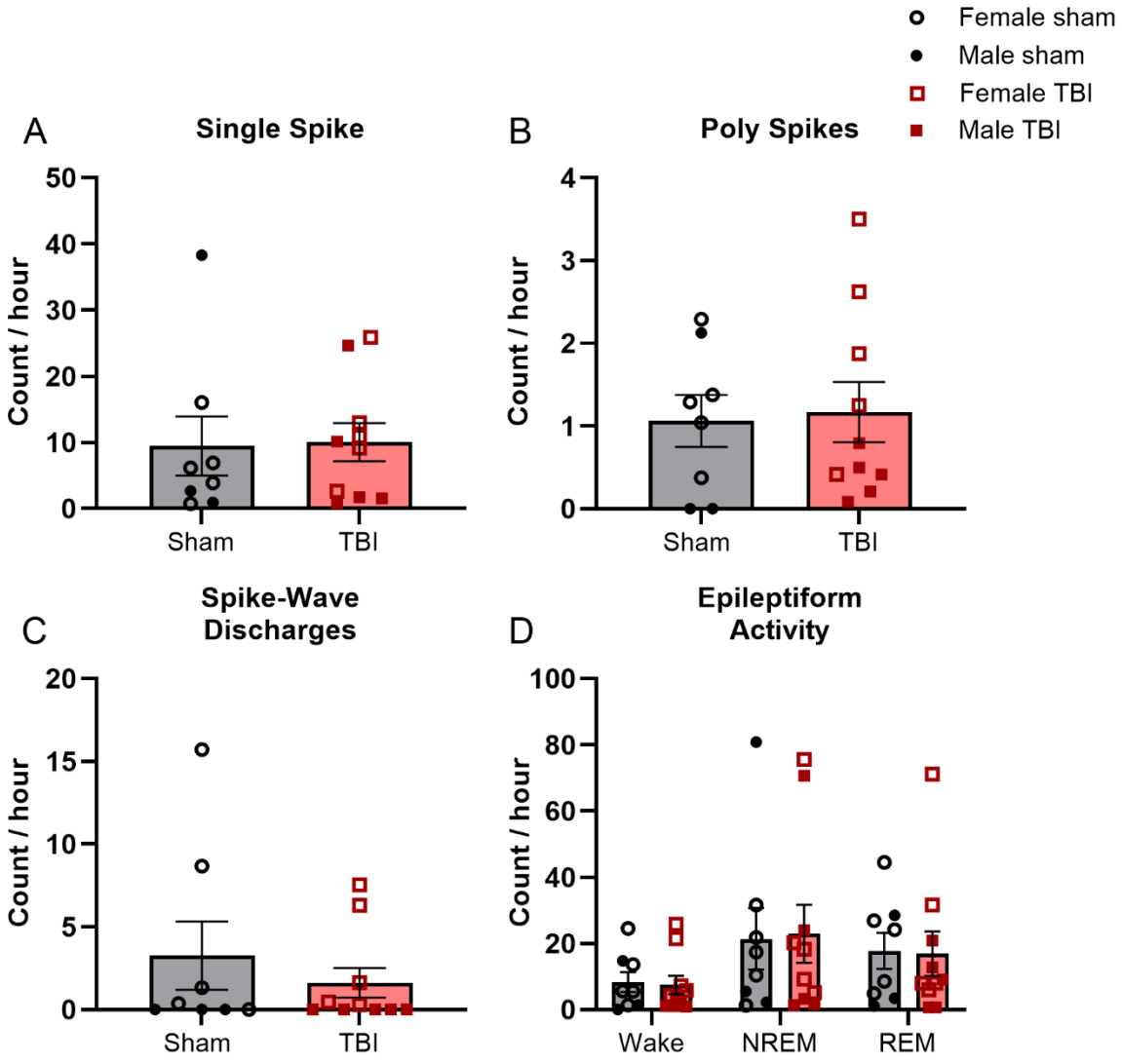

Figure 5. Epileptiform activity after rmTBI. (A) Single spike (SS) count per hour. **(B)** Poly-spikes (PS) count per hour. **(C)** Spike-Wave discharges (SWDs) count per hour. **(D)** Epileptiform activity (EA) count was obtained by adding SS, PS, and SWDs. Data are reported as mean ±SEM and analyzed by Mann Whitney-U test. Sham data are shown in black and rmTBI data are shown in red. Females are shown with open symbols and males are shown with solid symbols. Each data point represents the average for a single mouse. Male TBI n=5, male sham n=3; female TBI n=5, female sham n=5.

rmTBI induced neurological injury

We assessed the release of two cytoskeletal proteins, Nf-L from neurons and GFAP from astroglia, by performing a sandwich-ELISA-based MSD immunoassay using the blood plasma collected one month post-injury. Both proteins are highly sensitive biomarkers that can indicate neurological injury in the clinical diagnosis of TBI (Graham et al., 2021; Shahim et al., 2020). Two mice were removed due to failure to collect blood. We found that rmTBI was associated with a higher level of plasma Nf-L relative to the sham (p=0.0206) (Fig. 6A), but that plasma GFAP was not different between rmTBI and sham at this post-injury time point (p=0.6730) (Fig. 6B). These findings indicate that the CHIMERA rmTBI paradigm here induced enduring neurological injury in mice without markedly affecting brain inflammation.

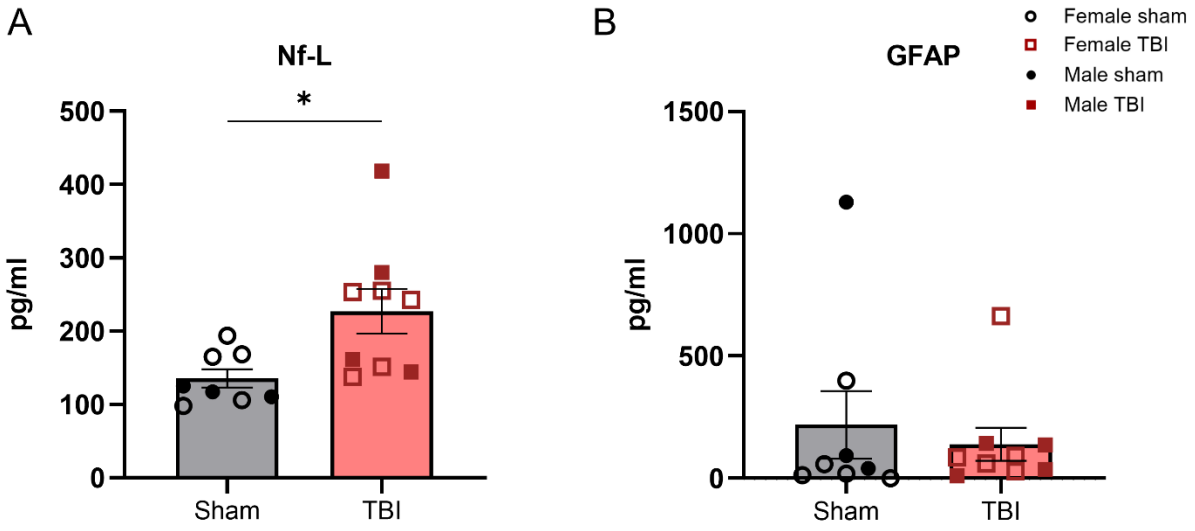

Figure 6. Plasma biomarkers after rmTBI. (A) Plasma Nf-L and **(B)** GFAP were compared between sham and TBI cohorts. Biomarker results were reported as mean ± SEM and analyzed by Mann Whitney-U test. Sham data are shown in black and rmTBI data are shown in red. Females are shown with open symbols and males are shown with solid symbols. Each data point represents a sample from a single mouse. Male TBI n=4, male sham n=3; female TBI n=5, female sham n=5. * $p < 0.05$.

Amyloid histopathology is not exacerbated one month post-injury

To determine whether rmTBI exacerbates amyloid burden in the brain one month post-injury, we performed immunohistochemistry using the anti-Aβ antibody 6E10 to analyze amyloid histopathology. One female mouse was removed from histological analysis due to excessive tissue

damage at cryosection. Overall, we found no differences in the level of amyloid plaques within the parietal isocortex and the hippocampus (Fig. 7A-C) after rmTBI, although amyloid pathology in females was significantly higher than in males in the isocortex (p=0.0177) (Fig. 7B). We also analyzed regional amyloid pathology within several isolated cortical regions based on a published report (Vasciaveo et al., 2023), but again, we found no differences in the percentage area of amyloid plaques induced by rmTBI (Supplementary Fig. S4). There were also no group differences in the level of amyloid plaques in the anterior cortical regions (i.e., the site of injury; Supplementary Fig. S5).

Additionally, we quantified the global level of soluble and insoluble monomeric $A\beta_{42}$ in the carbonic and GuHCl fractions of the whole brain lysate by ELISA. Again, we did not observe significant differences in the level of $A\beta_{42}$ (p>0.05) in both fractions, but a higher level of soluble $A\beta_{42}$ (p=0.0202) and an uptrend in the level of insoluble $A\beta_{42}$ (p=0.0744) were apparent in the female cohort regardless of injury (Fig 7 D-E), indicating a sex-dependent accumulation of $A\beta_{42}$ monomer in the brain. Altogether, the neuropathological data suggested that rmTBI did not significantly alter amyloid pathology one month post-injury in the APP/PS1 mice.

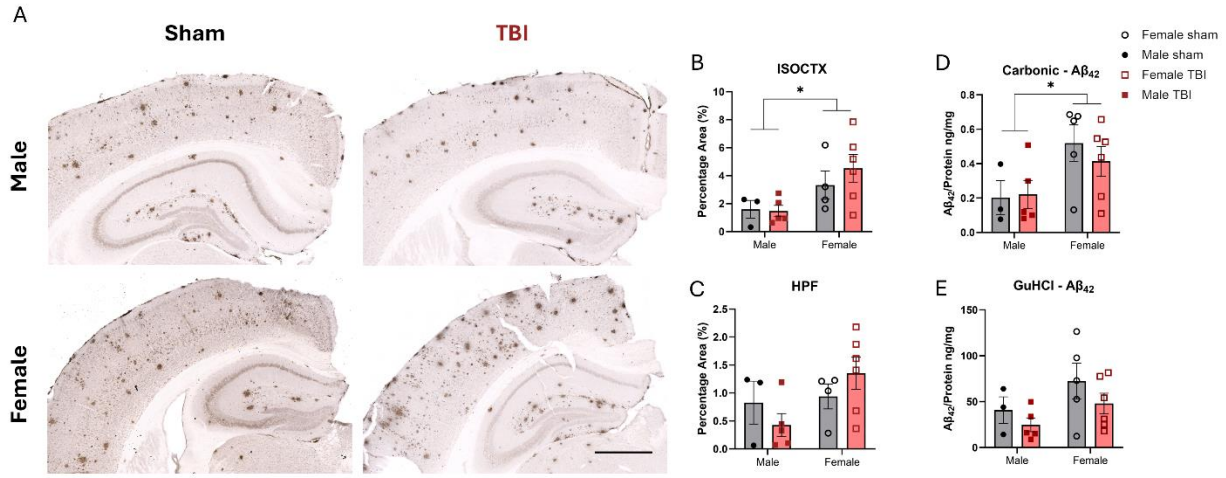

Figure 7. Amyloid pathology and Aβ42 after rmTBI. Amyloid plaques were immunostained by 6E10 one month post-injury. **(A)** Representative images of the isocortex and hippocampus of both male and female are shown. Scale bar = 1000 µm. Quantification of the percentage area of plaques in the **(B)** isocortex and **(C)** hippocampus of both sexes are shown on the right. Each data point represents the average of three sections per animal. Quantification of the **(D)** carbonic (soluble) and **(E)** GuHCl (insoluble) fractions of Aβ42 by ELISA using whole brain lysates. Each data point represents the average of three replicates per animal. Both histological and ELISA data are reported as mean ± SEM and analyzed by two-way ANOVA. Sham data are shown in black and rmTBI data are shown in red. Females are shown with open symbols and males are shown with solid symbols. For IHC, male TBI n=5, male sham n=3; female TBI n=6, female sham n=4. For ELISA, male TBI n=5, male sham n=3; female TBI n=6, female sham n=5. * p<0.05.

Discussion

Mild TBI is the most prevalent type of TBI and is associated with increased risk of neurodegenerative disease, particularly when more than one injury is experienced. The changes in sleep and epileptiform activity that have been reported after mTBI have been proposed to accelerate the progression of neurodegenerative processes. To explore the mechanisms underlying such changes, we characterized the effects of rmTBI on sleep, epileptiform activity, and amyloid pathology one month post-injury in a well-characterized mouse model of AD.

Using CHIMERA, we showed that rmTBI causes prolonged recovery in later injuries, which is associated with sustained neuronal damage in the APP/PS1 mice one month post-injury. RmTBI was also associated with a shift in the EEG power spectra during NREM sleep. However, no effects of rmTBI on vigilance state duration, epileptiform activity, or amyloid pathology were observed. We did observe the anticipated sex difference in amyloid burden, with females exhibiting higher levels in both aggregates and monomers. Females also exhibited more epileptiform activity than males.

Sleep disturbances, commonly experienced by concussed patients, have been linked to earlier onset of mild cognitive impairments and increased Aβ burden in the AD population (Holth et al., 2017; Mander et al., 2016; Nguyen Ho et al., 2024; Roh et al., 2012). Sleep fragmentation, linked to decreased slow-wave and REM sleep, has been associated with slower recovery after TBI (Fleming et al., 2020) and greater Aβ burden (Nguyen Ho et al., 2024) in humans, and is shown to suppress glymphatic function in mice(Deng et al., 2024). In this study, we did not observe enduring changes in total sleep or sleep fragmentation measures (transitions or bout lengths) induced by rmTBI, suggesting that sleep architecture is unaffected in the APP/PS1 mice at one month post rmTBI. Previous animal studies show mixed results on the effects of mTBI on sleep (Korthas et al., 2022; Portillo et al., 2023; Sandsmark et al., 2017). This is likely due to the differences in the TBI models and the duration post-injury. Notably, Rowe et al. (2014) showed that changes in sleep patterns caused by a midline fluid percussion injury could fade one week after injury, which supports the lack of changes in sleep in our cohort one month post-injury.

We also evaluated EEG spectral power, since it allows for further characterization of quantitative aspects of EEG. Typically, lower frequencies are dominant during NREM sleep, indicating a slowing down of brain activity and increased synchronization across brain areas. In contrast, higher frequencies are dominant during wake and indicate an increase in faster and more localized brain activity. Even though changes in sleep state duration were not observed in this cohort, our results show a shift in the spectral power density towards higher frequencies in the rmTBI group. This shift is characterized by a power reduction at the lower frequencies and a power increase at the higher frequencies compared to sham mice during NREM sleep. The spectral power shift could indicate poorer sleep quality and a reduction in slow wave activity in the rmTBI group during NREM. In human studies, decreased slow wave activity has been linked to impaired amyloid clearance and cognitive deficits (Chen et al., 2023; Ju et al., 2017; Winer et al., 2020). A reduction of lower frequencies, otherwise known as slow-wave sleep, has also been reported in humans with mild cognitive impairment and mild to moderate AD (Kent et al., 2022; Liguori et al., 2020; Liu et al., 2020).

In our study, the spectral shift was observed in the parietal electrode. This is perhaps due to the impact site being located in the midline of the parietal region. Most studies assessing quantitative

EEG after brain injury show an increase in slow-wave frequencies during wake with no changes occurring during NREM, both in mice and humans (Konduru et al., 2021; Modarres et al., 2017; Sandsmark et al., 2017). However, studies investigating sleep in AD transgenic mice have shown spectral power changes similar to the ones found in this study, mainly a shift towards higher frequencies during NREM (Kent et al., 2018, 2019; Zhang et al., 2019). The present study showed that this shift is exacerbated after rmTBI in APP/PS1 mice at 7 months old. We speculate that this shift could be part of early pathological changes in sleep that are modulated by rmTBI injury. This seems to be independent of Aβ plaque accumulation, epileptiform activity, or sleep stage changes. Further animal and human studies should investigate this shift in power spectra and the neuronal mechanisms causing it.

TBI has also been linked to post-traumatic epilepsy, potentially driven by increased iron levels, accumulation of glutamate, impaired axonal transport, neurotransmitter imbalances, and epigenetic modifications that contribute to neuronal excitotoxicity (Golub & Reddy, 2022). All of these changes lead to pathologic EEG activity such as high-frequency oscillations, abnormal sleep spindles, and epileptiform discharges, such as spikes and spike-wave discharges (Golub & Reddy, 2022). Ultimately, if neuronal hyperactivity persists, it can develop into seizures. In this study, we analyzed certain measures of neuronal hyperactivity (spikes, SWDs, and seizures) after rmTBI. There were no changes induced by rmTBI in the amount of epileptiform activity. It is noteworthy that the sham group tended to have higher variability than the rmTBI group, especially in single spikes and SWDs. This could be an intrinsic artifact of the APP/PS1 mouse line, which has been shown to have higher baseline levels of epileptiform activity compared to wild-type mice (Gureviciene et al., 2019; Minkeviciene et al., 2009; Reyes-Marin & Nuñez, 2017). Researchers have proposed that overexpression of APP and, as a direct result, a premature increase in amyloid β could be responsible for this increase in epileptiform activity (Hijazi et al., 2023; Minkeviciene et al., 2009; Palop et al., 2007; Tok, Ahnaou, et al., 2022; Verret et al., 2012). However, higher variability in the sham group could also be due to the smaller sample size of this group and the unbalanced male-to-female ratio. In our study, we also found that female mice were more vulnerable to epileptiform activity, with SWDs only observed in females. This is relevant since Nygaard et al. (2015) found that SWDs were correlated with impairments in spatial memory, and that brivaracetam treatment was successful at reducing SWDs and reversing memory impairments. This finding supports the inclusion of sex differences in pharmaceutical studies for AD and epilepsy treatment.

Another main finding in this study is that rmTBI induced and sustained an elevated level of Nf-L in plasma, which is indicative of neurological injury one month post-injury. This is consistent with clinical findings showing that the increases in plasma Nf-L correlate with the severity of TBI suffered by patients within five years (Shahim et al., 2020), as well as preclinical findings showing an increase in plasma Nf-L up to 5 weeks after closed-head mild-TBI (Moro et al., 2023). In contrast, we did not detect major differences in plasma GFAP between our sham and TBI cohorts at the investigated time point. To our knowledge, this is the first study reporting plasma GFAP at one month post-injury in a TBI animal model, when most preclinical studies report plasma GFAP levels within several hours to up to seven days post-injury (Cikriklar et al., 2015; Kmeťová et al., 2022; Lafrenaye et al., 2020; Wei et al., 2021). Clinical utility of plasma GFAP as a biomarker for TBI diagnosis appears limited to twelve months post-injury (Bogoslovsky et al., 2017; Gardner et al., 2022; Graham et al., 2021; Metting et al., 2012; Papa et al., 2014). A longitudinal profiling of the level of plasma GFAP in preclinical TBI models and TBI patients would provide a

comprehensive outlook on how plasma GFAP may be utilized as a diagnostic tool for assessing chronic brain injury.

Proteopathic changes have been reported in TBI patients months after TBI. Positron emission tomography (PET) imaging with the ^{11}C-PiB tracer suggested regional accumulation of amyloid plaques one year after a moderate-to-severe TBI (Scott et al., 2016). Several groups have also reported that TBI is associated with protein aggregation related to AD in animal models (Alyenbaawi et al., 2021; Edwards et al., 2020; Washington et al., 2014). However, how repetitive-mild TBIs alter protein aggregation in mice remains unclear. Although we found no significant changes in the level of amyloid pathology in the APP/PS1 mice one month after rmTBI, others have suggested that the age of onset for amyloidosis in the transgenic APP mouse model may dictate the amyloidogenic outcome driven by TBI. For instance, reduced amyloid plaques below basal level have been reported in several transgenic APP mouse strains after receiving TBI at or beyond six months of age by using the controlled cortical impact (Nakagawa et al., 2000), the lateral fluid percussion injury (Collins et al., 2019), and most relevant to our study, the CHIMERA (Cheng et al., 2019). This is perhaps due to changes in the clearance or enzymatic processing of Aβ after injury in older mice, where amyloid pathology has already been established. We also observed a high heterogeneity in the deposition of amyloid plaques at the investigated age in our cohort (Fig 7), indicating high variability in the basal level of amyloid pathology (Yan et al., 2009). Based on these reports and our findings, we speculate that inducing rmTBI by CHIMERA in the APP/PS1 mice at younger ages prior to the onset of amyloidosis may manifest injury effects on amyloid pathology.

There are other potential limitations in the present study. First, the current TBI paradigm only delivers low energy impacts within one week, which may be insufficient to induce other injury responses. Second, the heterogeneity in body physique between male and female mice may require further optimization of the intensity of TBI, such as adjusting the energy and frequency of impacts, with references from blood biomarkers such as Nf-L, or behavioural deficits, to ensure both cohorts undergo similar levels of brain injury. Lastly, this study might be underpowered to detect smaller effects that could be present at one month post-injury. Nevertheless, our study demonstrates a feasible framework for the characterization of the electrophysiological, pathohistological, and plasma biomarkers following mTBI in a mouse model of AD, to enhance the exploration of the underlying mechanism of repetitive TBI driving the pathogenicity of AD in humans.

Acknowledgement

We thank Samantha Saw, Japneet Kaur, Bonnie K. Ng, Mayuko Arai and Robert Gibson for assisting in *in vivo* procedures and immunohistochemistry. We thank Dr. Sarah Faber for her insightful advice on power spectra analysis. We thank the SFU animal research facility for maintaining the animals used in this study.

References

Alyenbaawi, H., Kanyo, R., Locskai, L. F., Kamali-Jamil, R., DuVal, M. G., Bai, Q., Wille, H., Burton, E. A., & Allison, W. T. (2021). Seizures are a druggable mechanistic link between TBI and subsequent tauopathy. *eLife*, *10*, e58744. https://doi.org/10.7554/eLife.58744

Aoun, R., Rawal, H., Attarian, H., & Sahni, A. (2019). Impact of traumatic brain injury on sleep: An overview. *Nature and Science of Sleep, Volume 11*, 131–140. https://doi.org/10.2147/NSS.S182158

Berman, R., Spencer, H., Boese, M., Kim, S., Radford, K., & Choi, K. (2023). Loss of Consciousness and Righting Reflex Following Traumatic Brain Injury: Predictors of Post-Injury Symptom Development (A Narrative Review). *Brain Sciences*, *13*(5), 750. https://doi.org/10.3390/brainsci13050750

Bogoslovsky, T., Wilson, D., Chen, Y., Hanlon, D., Gill, J., Jeromin, A., Song, L., Moore, C., Gong, Y., Kenney, K., & Diaz-Arrastia, R. (2017). Increases of Plasma Levels of Glial Fibrillary Acidic Protein, Tau, and Amyloid β up to 90 Days after Traumatic Brain Injury. *Journal of Neurotrauma*, *34*(1), 66–73. https://doi.org/10.1089/neu.2015.4333

Bugay, V., Bozdemir, E., Vigil, F. A., Chun, S. H., Holstein, D. M., Elliott, W. R., Sprague, C. J., Cavazos, J. E., Zamora, D. O., Rule, G., Shapiro, M. S., Lechleiter, J. D., & Brenner, R. (2020). A Mouse Model of Repetitive Blast Traumatic Brain Injury Reveals Post-Trauma Seizures and Increased Neuronal Excitability. *Journal of Neurotrauma*, *37*(2), 248–261. https://doi.org/10.1089/neu.2018.6333

Button, E. B., Cheng, W. H., Barron, C., Cheung, H., Bashir, A., Cooper, J., Gill, J., Stukas, S., Baron, D. C., Robert, J., Rowe, E. M., Cripton, P. A., & Wellington, C. L. (2021). Development of a novel, sensitive translational immunoassay to detect plasma glial

fibrillary acidic protein (GFAP) after murine traumatic brain injury. *Alzheimer's Research & Therapy*, *13*(1), 58. https://doi.org/10.1186/s13195-021-00793-9

Chen, C.-W., Kwok, Y.-T., Cheng, Y.-T., Huang, Y.-S., Kuo, T. B. J., Wu, C.-H., Du, P.-J., Yang, A. C., & Yang, C. C. H. (2023). Reduced slow-wave activity and autonomic dysfunction during sleep precede cognitive deficits in Alzheimer's disease transgenic mice. *Scientific Reports*, *13*(1). https://doi.org/10.1038/s41598-023-38214-6

Cheng, W. H., Martens, K. M., Bashir, A., Cheung, H., Stukas, S., Gibbs, E., Namjoshi, D. R., Button, E. B., Wilkinson, A., Barron, C. J., Cashman, N. R., Cripton, P. A., & Wellington, C. L. (2019). CHIMERA repetitive mild traumatic brain injury induces chronic behavioural and neuropathological phenotypes in wild-type and APP/PS1 mice. *Alzheimer's Research & Therapy*, *11*(1), 6. https://doi.org/10.1186/s13195-018-0461-0

Cheng, W. H., Stukas, S., Martens, K. M., Namjoshi, D. R., Button, E. B., Wilkinson, A., Bashir, A., Robert, J., Cripton, P. A., & Wellington, C. L. (2018). Age at injury and genotype modify acute inflammatory and neurofilament-light responses to mild CHIMERA traumatic brain injury in wild-type and APP/PS1 mice. *Experimental Neurology*, *301*, 26–38. https://doi.org/10.1016/j.expneurol.2017.12.007

Cikriklar, H. I., Onur, U., Ekici, M. A., Ozbek, Z., Cosan, D. T., Yucel, M., Yurumez, Y., & Baydemir, C. (2015). Effectiveness of gfap in determining neuron damage in rats with induced head trauma. *Turkish Neurosurgery*. https://doi.org/10.5137/1019-5149.JTN.13946-15.2

Collins, J. M., King, A. E., Woodhouse, A., Kirkcaldie, M. T. K., & Vickers, J. C. (2019). Age Moderates the Effects of Traumatic Brain Injury on Beta-Amyloid Plaque Load in

APP/PS1 Mice. *Journal of Neurotrauma*, *36*(11), 1876–1889. https://doi.org/10.1089/neu.2018.5982

Conte, V., Uryu, K., Fujimoto, S., Yao, Y., Rokach, J., Longhi, L., Trojanowski, J. Q., Lee, V. M., McIntosh, T. K., & Praticò, D. (2004). Vitamin E reduces amyloidosis and improves cognitive function in Tg2576 mice following repetitive concussive brain injury. *Journal of Neurochemistry*, *90*(3), 758–764. https://doi.org/10.1111/j.1471-4159.2004.02560.x

Cragg, L., Kovacevic, N., McIntosh, A. R., Poulsen, C., Martinu, K., Leonard, G., & Paus, T. (2011). Maturation of EEG power spectra in early adolescence: A longitudinal study: Maturation of EEG. *Developmental Science*, *14*(5), 935–943. https://doi.org/10.1111/j.1467-7687.2010.01031.x

Deng, S., Hu, Y., Chen, S., Xue, Y., Yao, D., Sun, Q., Nedergaard, M., Wang, W., & Ding, F. (2024). Chronic sleep fragmentation impairs brain interstitial clearance in young wildtype mice. *Journal of Cerebral Blood Flow & Metabolism*, *44*(9), 1515–1531. https://doi.org/10.1177/0271678X241230188

Edwards, G., Zhao, J., Dash, P. K., Soto, C., & Moreno-Gonzalez, I. (2020). Traumatic Brain Injury Induces Tau Aggregation and Spreading. *Journal of Neurotrauma*, *37*(1), 80–92. https://doi.org/10.1089/neu.2018.6348

Fleming, M. K., Smejka, T., Henderson Slater, D., van Gils, V., Garratt, E., Yilmaz Kara, E., & Johansen-Berg, H. (2020). Sleep Disruption After Brain Injury Is Associated With Worse Motor Outcomes and Slower Functional Recovery. *Neurorehabilitation and Neural Repair*, *34*(7), 661–671. https://doi.org/10.1177/1545968320929669

Gardner, R. C., Puccio, A. M., Korley, F. K., Wang, K. K. W., Diaz-Arrastia, R., Okonkwo, D. O., Puffer, R. C., Yuh, E. L., Yue, J. K., Sun, X., Taylor, S. R., Mukherjee, P., Jain, S.,

Manley, G. T., the TRACK-TBI Investigators, Feeser, V. R., Ferguson, A. R., Gaudette, E., Gopinath, S., … Zafonte, R. (2022). Effects of age and time since injury on traumatic brain injury blood biomarkers: A TRACK-TBI study. *Brain Communications*, *5*(1), fcac316. https://doi.org/10.1093/braincomms/fcac316

Golden, C. J., & Zusman, M. R. (2019). Clinical Manifestations of CTE: Disruptions in Cognition, Mood, & Behavior. In C. J. Golden & M. R. Zusman, *Chronic Traumatic Encephalopathy (CTE)* (pp. 11–38). Springer International Publishing. https://doi.org/10.1007/978-3-030-23288-7_2

Golub, V. M., & Reddy, D. S. (2022). Post-Traumatic Epilepsy and Comorbidities: Advanced Models, Molecular Mechanisms, Biomarkers, and Novel Therapeutic Interventions. *Pharmacological Reviews*, *74*(2), 387–438. https://doi.org/10.1124/pharmrev.121.000375

Graham, N. S. N., Zimmerman, K. A., Moro, F., Heslegrave, A., Maillard, S. A., Bernini, A., Miroz, J.-P., Donat, C. K., Lopez, M. Y., Bourke, N., Jolly, A. E., Mallas, E.-J., Soreq, E., Wilson, M. H., Fatania, G., Roi, D., Patel, M. C., Garbero, E., Nattino, G., … Sharp, D. J. (2021). Axonal marker neurofilament light predicts long-term outcomes and progressive neurodegeneration after traumatic brain injury. *Science Translational Medicine*, *13*(613), eabg9922. https://doi.org/10.1126/scitranslmed.abg9922

Gureviciene, I., Ishchenko, I., Ziyatdinova, S., Jin, N., Lipponen, A., Gurevicius, K., & Tanila, H. (2019). Characterization of Epileptic Spiking Associated With Brain Amyloidosis in APP/PS1 Mice. *Frontiers in Neurology*, *10*, 1151. https://doi.org/10.3389/fneur.2019.01151

Guskiewicz, K. M., McCrea, M., Marshall, S. W., Cantu, R. C., Randolph, C., Barr, W., Onate, J. A., & Kelly, J. P. (2003). Cumulative Effects Associated With Recurrent Concussion in

Collegiate Football Players: The NCAA Concussion Study. *JAMA*, *290*(19), 2549. https://doi.org/10.1001/jama.290.19.2549

Hijazi, S., Smit, A. B., & Van Kesteren, R. E. (2023). Fast-spiking parvalbumin-positive interneurons in brain physiology and Alzheimer's disease. *Molecular Psychiatry*, *28*(12), 4954–4967. https://doi.org/10.1038/s41380-023-02168-y

Holth, J. K., Mahan, T. E., Robinson, G. O., Rocha, A., & Holtzman, D. M. (2017). Altered sleep and EEG power in the P301S Tau transgenic mouse model. *Annals of Clinical and Translational Neurology*, *4*(3), 180–190. https://doi.org/10.1002/acn3.390

Howlett, J. R., Nelson, L. D., & Stein, M. B. (2022). Mental Health Consequences of Traumatic Brain Injury. *Biological Psychiatry*, *91*(5), 413–420. https://doi.org/10.1016/j.biopsych.2021.09.024

Jankowsky, J. L., Slunt, H. H., Ratovitski, T., Jenkins, N. A., Copeland, N. G., & Borchelt, D. R. (2001). Co-expression of multiple transgenes in mouse CNS: A comparison of strategies. *Biomolecular Engineering*, *17*(6), 157–165. https://doi.org/10.1016/S1389-0344(01)00067-3

Jin, N., Babiloni, C., Drinkenburg, W. H., Hajós, M., Nygaard, H. B., & Tanila, H. (2022). Recommendations for Preclinical Testing of Treatments Against Alzheimer's Disease-Related Epileptiform Spikes in Transgenic Rodent Models. *Journal of Alzheimer's Disease: JAD*, *88*(3), 849–865. https://doi.org/10.3233/JAD-210209

Ju, Y.-E. S., Ooms, S. J., Sutphen, C., Macauley, S. L., Zangrilli, M. A., Jerome, G., Fagan, A. M., Mignot, E., Zempel, J. M., Claassen, J. A. H. R., & Holtzman, D. M. (2017). Slow wave sleep disruption increases cerebrospinal fluid amyloid-β levels. *Brain*, *140*(8), 2104–2111. https://doi.org/10.1093/brain/awx148

Karr, J. E., Areshenkoff, C. N., & Garcia-Barrera, M. A. (2014). The neuropsychological outcomes of concussion: A systematic review of meta-analyses on the cognitive sequelae of mild traumatic brain injury. *Neuropsychology*, *28*(3), 321–336. https://doi.org/10.1037/neu0000037

Kent, B. A., Casciola, A. A., Carlucci, S. K., Chen, M., Stager, S., Mirian, M. S., Slack, P., Valerio, J., McKeown, M. J., Feldman, H. H., & Nygaard, H. B. (2022). Home EEG sleep assessment shows reduced slow-wave sleep in mild–moderate Alzheimer's disease. *Alzheimer's & Dementia: Translational Research & Clinical Interventions*, *8*(1), e12347. https://doi.org/10.1002/trc2.12347

Kent, B. A., Feldman, H. H., & Nygaard, H. B. (2021). Sleep and its regulation: An emerging pathogenic and treatment frontier in Alzheimer's disease. *Progress in Neurobiology*, *197*, 101902. https://doi.org/10.1016/j.pneurobio.2020.101902

Kent, B. A., Michalik, M., Marchant, E. G., Yau, K. W., Feldman, H. H., Mistlberger, R. E., & Nygaard, H. B. (2019). Delayed daily activity and reduced NREM slow-wave power in the APPswe/PS1dE9 mouse model of Alzheimer's disease. *Neurobiology of Aging*, *78*, 74–86. https://doi.org/10.1016/j.neurobiolaging.2019.01.010

Kent, B. A., Strittmatter, S. M., & Nygaard, H. B. (2018). Sleep and EEG Power Spectral Analysis in Three Transgenic Mouse Models of Alzheimer's Disease: APP/PS1, 3xTgAD, and Tg2576. *Journal of Alzheimer's Disease*, *64*(4), 1325–1336. https://doi.org/10.3233/JAD-180260

Kmeťová, K., Drobná, D., Lipták, R., Hodosy, J., & Celec, P. (2022). Early dynamics of glial fibrillary acidic protein and extracellular DNA in plasma of mice after closed head

traumatic brain injury. *Neurochirurgie*, *68*(6), e68–e74. https://doi.org/10.1016/j.neuchi.2022.06.003

Konduru, S. S., Wallace, E. P., Pfammatter, J. A., Rodrigues, P. V., Jones, M. V., & Maganti, R. K. (2021). Sleep-wake characteristics in a mouse model of severe traumatic brain injury: Relation to posttraumatic epilepsy. *Epilepsia Open*, *6*(1), 181–194. https://doi.org/10.1002/epi4.12462

Korthas, H. T., Main, B. S., Harvey, A. C., Buenaventura, R. G., Wicker, E., Forcelli, P. A., & Burns, M. P. (2022). The Effect of Traumatic Brain Injury on Sleep Architecture and Circadian Rhythms in Mice—A Comparison of High-Frequency Head Impact and Controlled Cortical Injury. *Biology*, *11*(7), 1031. https://doi.org/10.3390/biology11071031

Lafrenaye, A. D., Mondello, S., Wang, K. K., Yang, Z., Povlishock, J. T., Gorse, K., Walker, S., Hayes, R. L., & Kochanek, P. M. (2020). Circulating GFAP and Iba-1 levels are associated with pathophysiological sequelae in the thalamus in a pig model of mild TBI. *Scientific Reports*, *10*(1), 13369. https://doi.org/10.1038/s41598-020-70266-w

Langford, D. J., Bailey, A. L., Chanda, M. L., Clarke, S. E., Drummond, T. E., Echols, S., Glick, S., Ingrao, J., Klassen-Ross, T., LaCroix-Fralish, M. L., Matsumiya, L., Sorge, R. E., Sotocinal, S. G., Tabaka, J. M., Wong, D., Van Den Maagdenberg, A. M. J. M., Ferrari, M. D., Craig, K. D., & Mogil, J. S. (2010). Coding of facial expressions of pain in the laboratory mouse. *Nature Methods*, *7*(6), 447–449. https://doi.org/10.1038/nmeth.1455

Lefevre-Dognin, C., Cogné, M., Perdrieau, V., Granger, A., Heslot, C., & Azouvi, P. (2021). Definition and epidemiology of mild traumatic brain injury. *Neurochirurgie*, *67*(3), 218–221. https://doi.org/10.1016/j.neuchi.2020.02.002

Liguori, C., Placidi, F., Izzi, F., Spanetta, M., Mercuri, N. B., & Di Pucchio, A. (2020). Sleep dysregulation, memory impairment, and CSF biomarkers during different levels of neurocognitive functioning in Alzheimer's disease course. *Alzheimer's Research & Therapy*, *12*(1), 5. https://doi.org/10.1186/s13195-019-0571-3

Liu, S., Pan, J., Tang, K., Lei, Q., He, L., Meng, Y., Cai, X., & Li, Z. (2020). Sleep spindles, K-complexes, limb movements and sleep stage proportions may be biomarkers for amnestic mild cognitive impairment and Alzheimer's disease. *Sleep and Breathing*, *24*(2), 637–651. https://doi.org/10.1007/s11325-019-01970-9

Maas, A. I. R., Menon, D. K., Manley, G. T., Abrams, M., Åkerlund, C., Andelic, N., Aries, M., Bashford, T., Bell, M. J., Bodien, Y. G., Brett, B. L., Büki, A., Chesnut, R. M., Citerio, G., Clark, D., Clasby, B., Cooper, D. J., Czeiter, E., Czosnyka, M., … Zemek, R. (2022). Traumatic brain injury: Progress and challenges in prevention, clinical care, and research. *The Lancet Neurology*, *21*(11), 1004–1060. https://doi.org/10.1016/S1474-4422(22)00309-X

Mander, B. A., Winer, J. R., Jagust, W. J., & Walker, M. P. (2016). Sleep: A Novel Mechanistic Pathway, Biomarker, and Treatment Target in the Pathology of Alzheimer's Disease? *Trends in Neurosciences*, *39*(8), 552–566. https://doi.org/10.1016/j.tins.2016.05.002

Massimini, M., Corbetta, M., Sanchez-Vives, M. V., Andrillon, T., Deco, G., Rosanova, M., & Sarasso, S. (2024). Sleep-like cortical dynamics during wakefulness and their network effects following brain injury. *Nature Communications*, *15*(1), 7207. https://doi.org/10.1038/s41467-024-51586-1

McIntosh, A. R., & Lobaugh, N. J. (2004). Partial least squares analysis of neuroimaging data: Applications and advances. *NeuroImage*, *23*, S250–S263. https://doi.org/10.1016/j.neuroimage.2004.07.020

Metting, Z., Wilczak, N., Rodiger, L. A., Schaaf, J. M., & Van Der Naalt, J. (2012). GFAP and S100B in the acute phase of mild traumatic brain injury. *Neurology*, *78*(18), 1428–1433. https://doi.org/10.1212/WNL.0b013e318253d5c7

Minkeviciene, R., Rheims, S., Dobszay, M. B., Zilberter, M., Hartikainen, J., Fülöp, L., Penke, B., Zilberter, Y., Harkany, T., Pitkänen, A., & Tanila, H. (2009). Amyloid β-Induced Neuronal Hyperexcitability Triggers Progressive Epilepsy. *The Journal of Neuroscience*, *29*(11), 3453–3462. https://doi.org/10.1523/JNEUROSCI.5215-08.2009

Mishra, P., Pandey, C., Singh, U., Gupta, A., Sahu, C., & Keshri, A. (2019). Descriptive statistics and normality tests for statistical data. *Annals of Cardiac Anaesthesia*, *22*(1), 67. https://doi.org/10.4103/aca.ACA_157_18

Modarres, M. H., Kuzma, N. N., Kretzmer, T., Pack, A. I., & Lim, M. M. (2017). EEG slow waves in traumatic brain injury: Convergent findings in mouse and man. *Neurobiology of Sleep and Circadian Rhythms*, *2*, 59–70. https://doi.org/10.1016/j.nbscr.2016.06.001

Montenigro, P. H., Alosco, M. L., Martin, B. M., Daneshvar, D. H., Mez, J., Chaisson, C. E., Nowinski, C. J., Au, R., McKee, A. C., Cantu, R. C., McClean, M. D., Stern, R. A., & Tripodis, Y. (2017). Cumulative Head Impact Exposure Predicts Later-Life Depression, Apathy, Executive Dysfunction, and Cognitive Impairment in Former High School and College Football Players. *Journal of Neurotrauma*, *34*(2), 328–340. https://doi.org/10.1089/neu.2016.4413

Moro, F., Lisi, I., Tolomeo, D., Vegliante, G., Pascente, R., Mazzone, E., Hussain, R., Micotti, E., Dallmeier, J., Pischiutta, F., Bianchi, E., Chiesa, R., Wang, K. K., & Zanier, E. R. (2023). Acute Blood Levels of Neurofilament Light Indicate One-Year White Matter Pathology and Functional Impairment in Repetitive Mild Traumatic Brain Injured Mice. *Journal of Neurotrauma*, *40*(11–12), 1144–1163. https://doi.org/10.1089/neu.2022.0252

Morris, A. R., Gudenschwager Basso, E. K., Gutierrez-Monreal, M. A., Arja, R. D., Kobeissy, F. H., Janus, C. G., Wang, K. K. W., Zhu, J., & Liu, A. C. (2024). Lifelong Chronic Sleep Disruption in a Mouse Model of Traumatic Brain Injury. *Neurotrauma Reports*, *5*(1), 61–73. https://doi.org/10.1089/neur.2023.0107

Nakagawa, Y., Reed, L., Nakamura, M., McIntosh, T. K., Smith, D. H., Saatman, K. E., Raghupathi, R., Clemens, J., Saido, T. C., Lee, V. M.-Y., & Trojanowski, J. Q. (2000). Brain Trauma in Aged Transgenic Mice Induces Regression of Established Aβ Deposits. *Experimental Neurology*, *163*(1), 244–252. https://doi.org/10.1006/exnr.2000.7375

Namjoshi, D. R., Cheng, W. H., Bashir, A., Wilkinson, A., Stukas, S., Martens, K. M., Whyte, T., Abebe, Z. A., McInnes, K. A., Cripton, P. A., & Wellington, C. L. (2017). Defining the biomechanical and biological threshold of murine mild traumatic brain injury using CHIMERA (Closed Head Impact Model of Engineered Rotational Acceleration). *Experimental Neurology*, *292*, 80–91. https://doi.org/10.1016/j.expneurol.2017.03.003

Namjoshi, D. R., Cheng, W. H., McInnes, K. A., Martens, K. M., Carr, M., Wilkinson, A., Fan, J., Robert, J., Hayat, A., Cripton, P. A., & Wellington, C. L. (2014). Merging pathology with biomechanics using CHIMERA (Closed-Head Impact Model of Engineered Rotational Acceleration): A novel, surgery-free model of traumatic brain injury. *Molecular Neurodegeneration*, *9*(1), 55. https://doi.org/10.1186/1750-1326-9-55

Nguyen Ho, P. T., Hoepel, S. J. W., Rodriguez-Ayllon, M., Luik, A. I., Vernooij, M. W., & Neitzel, J. (2024). Sleep, 24-Hour Activity Rhythms, and Subsequent Amyloid-β Pathology. *JAMA Neurology*, *81*(8), 824–834. https://doi.org/10.1001/jamaneurol.2024.1755

Nwakamma, M. C., Stillman, A. M., Gabard-Durnam, L. J., Cavanagh, J. F., Hillman, C. H., & Morris, T. P. (2024). Slowing of Parameterized Resting-State Electroencephalography After Mild Traumatic Brain Injury. *Neurotrauma Reports*, *5*(1), 448–461. https://doi.org/10.1089/neur.2024.0004

Nygaard, H. B., Kaufman, A. C., Sekine-Konno, T., Huh, L. L., Going, H., Feldman, S. J., Kostylev, M. A., & Strittmatter, S. M. (2015). Brivaracetam, but not ethosuximide, reverses memory impairments in an Alzheimer's disease mouse model. *Alzheimer's Research & Therapy*, *7*(1), 25. https://doi.org/10.1186/s13195-015-0110-9

Palop, J. J., Chin, J., Roberson, E. D., Wang, J., Thwin, M. T., Bien-Ly, N., Yoo, J., Ho, K. O., Yu, G.-Q., Kreitzer, A., Finkbeiner, S., Noebels, J. L., & Mucke, L. (2007). Aberrant Excitatory Neuronal Activity and Compensatory Remodeling of Inhibitory Hippocampal Circuits in Mouse Models of Alzheimer's Disease. *Neuron*, *55*(5), 697–711. https://doi.org/10.1016/j.neuron.2007.07.025

Papa, L., Silvestri, S., Brophy, G. M., Giordano, P., Falk, J. L., Braga, C. F., Tan, C. N., Ameli, N. J., Demery, J. A., Dixit, N. K., Mendes, M. E., Hayes, R. L., Wang, K. K. W., & Robertson, C. S. (2014). GFAP Out-Performs S100β in Detecting Traumatic Intracranial Lesions on Computed Tomography in Trauma Patients with Mild Traumatic Brain Injury and Those with Extracranial Lesions. *Journal of Neurotrauma*, *31*(22), 1815–1822. https://doi.org/10.1089/neu.2013.3245

Petraglia, A. L., Plog, B. A., Dayawansa, S., Chen, M., Dashnaw, M. L., Czerniecka, K., Walker, C. T., Viterise, T., Hyrien, O., Iliff, J. J., Deane, R., Nedergaard, M., & Huang, J. H. (2014). The Spectrum of Neurobehavioral Sequelae after Repetitive Mild Traumatic Brain Injury: A Novel Mouse Model of Chronic Traumatic Encephalopathy. *Journal of Neurotrauma*, *31*(13), 1211–1224. https://doi.org/10.1089/neu.2013.3255

Portillo, E., Zi, X., Kim, Y., Tucker, L. B., Fu, A., Miller, L. A., Valenzuela, K. S., Sullivan, G. M., Gauff, A. K., Yu, F., Radomski, K. L., McCabe, J. T., & Armstrong, R. C. (2023). Persistent hypersomnia following repetitive mild experimental traumatic brain injury: Roles of chronic stress and sex differences. *Journal of Neuroscience Research*, *101*(6), 843–865. https://doi.org/10.1002/jnr.25165

Reyes-Marin, K. E., & Nuñez, A. (2017). Seizure susceptibility in the APP/PS1 mouse model of Alzheimer's disease and relationship with amyloid β plaques. *Brain Research*, *1677*, 93–100. https://doi.org/10.1016/j.brainres.2017.09.026

Roh, J. H., Huang, Y., Bero, A. W., Kasten, T., Stewart, F. R., Bateman, R. J., & Holtzman, D. M. (2012). Disruption of the Sleep-Wake Cycle and Diurnal Fluctuation of β-Amyloid in Mice with Alzheimer's Disease Pathology. *Science Translational Medicine*, *4*(150), 150ra122-150ra122. https://doi.org/10.1126/scitranslmed.3004291

Rowe, R. K., Harrison, J. L., O'Hara, B. F., & Lifshitz, J. (2014). Diffuse brain injury does not affect chronic sleep patterns in the mouse. *Brain Injury*, *28*(4), 504–510. https://doi.org/10.3109/02699052.2014.888768

Saletti, P. G., Katsarou, A. M., Molero, M., & Galanopoulou, A. S. (2021). Neurobiological Aspects of Post-traumatic Epilepsy: Lessons from Animal Models. In M. Mula (Ed.),

Post-traumatic Epilepsy (1st ed., pp. 1–28). Cambridge University Press. https://doi.org/10.1017/9781108644594.003

Sandsmark, D. K., Elliott, J. E., & Lim, M. M. (2017). Sleep-Wake Disturbances After Traumatic Brain Injury: Synthesis of Human and Animal Studies. *Sleep*, *40*(5), zsx044. https://doi.org/10.1093/sleep/zsx044

Scott, G., Ramlackhansingh, A. F., Edison, P., Hellyer, P., Cole, J., Veronese, M., Leech, R., Greenwood, R. J., Turkheimer, F. E., Gentleman, S. M., Heckemann, R. A., Matthews, P. M., Brooks, D. J., & Sharp, D. J. (2016). Amyloid pathology and axonal injury after brain trauma. *Neurology*, *86*(9), 821–828. https://doi.org/10.1212/WNL.0000000000002413

Shahim, P., Politis, A., Van Der Merwe, A., Moore, B., Chou, Y.-Y., Pham, D. L., Butman, J. A., Diaz-Arrastia, R., Gill, J. M., Brody, D. L., Zetterberg, H., Blennow, K., & Chan, L. (2020). Neurofilament light as a biomarker in traumatic brain injury. *Neurology*, *95*(6). https://doi.org/10.1212/WNL.0000000000009983

Shandra, O., Winemiller, A. R., Heithoff, B. P., Munoz-Ballester, C., George, K. K., Benko, M. J., Zuidhoek, I. A., Besser, M. N., Curley, D. E., Edwards, G. F., Mey, A., Harrington, A. N., Kitchen, J. P., & Robel, S. (2019). Repetitive Diffuse Mild Traumatic Brain Injury Causes an Atypical Astrocyte Response and Spontaneous Recurrent Seizures. *Journal of Neuroscience*, *39*(10), 1944–1963. https://doi.org/10.1523/JNEUROSCI.1067-18.2018

Theadom, A., Mahon, S., Hume, P., Starkey, N., Barker-Collo, S., Jones, K., Majdan, M., & Feigin, V. L. (2020). Incidence of Sports-Related Traumatic Brain Injury of All Severities: A Systematic Review. *Neuroepidemiology*, *54*(2), 192–199. https://doi.org/10.1159/000505424

Tok, S., Ahnaou, A., & Drinkenburg, W. (2022). Functional Neurophysiological Biomarkers of Early-Stage Alzheimer's Disease: A Perspective of Network Hyperexcitability in Disease Progression. *Journal of Alzheimer's Disease*, *88*(3), 809–836. https://doi.org/10.3233/jad-210397

Tok, S., Crauwels, D., & Drinkenburg, W. (2022). A Characterization of Epileptiform Activity Associated with TAU Seeding and Amyloid Pathology in the APPKM670/671NL.PS1/L166P and APP-KI Animal Models. *Journal of Neurology and Experimental Neuroscience*, *08*(01). https://doi.org/10.17756/jnen.2022-096

Uryu, K., Laurer, H., McIntosh, T., Praticò, D., Martinez, D., Leight, S., Lee, V. M.-Y., & Trojanowski, J. Q. (2002). Repetitive Mild Brain Trauma Accelerates Aβ Deposition, Lipid Peroxidation, and Cognitive Impairment in a Transgenic Mouse Model of Alzheimer Amyloidosis. *Journal of Neuroscience*, *22*(2), 446–454. https://doi.org/10.1523/JNEUROSCI.22-02-00446.2002

Van Den Heuvel, C., Thornton, E., & Vink, R. (2007). Traumatic brain injury and Alzheimer's disease: A review. In J. T. Weber & A. I. R. Maas (Eds.), *Progress in Brain Research* (Vol. 161, pp. 303–316). Elsevier. https://doi.org/10.1016/S0079-6123(06)61021-2

Vasciaveo, V., Iadarola, A., Casile, A., Dante, D., Morello, G., Minotta, L., Tamagno, E., Cicolin, A., & Guglielmotto, M. (2023). Sleep fragmentation affects glymphatic system through the different expression of AQP4 in wild type and 5xFAD mouse models. *Acta Neuropathologica Communications*, *11*(1), 16. https://doi.org/10.1186/s40478-022-01498-2

Verret, L., Mann, E. O., Hang, G. B., Barth, A. M. I., Cobos, I., Ho, K., Devidze, N., Masliah, E., Kreitzer, A. C., Mody, I., Mucke, L., & Palop, J. J. (2012). Inhibitory Interneuron

Deficit Links Altered Network Activity and Cognitive Dysfunction in Alzheimer Model. *Cell*, *149*(3), 708–721. https://doi.org/10.1016/j.cell.2012.02.046

Vossel, K. A., Tartaglia, M. C., Nygaard, H. B., Zeman, A. Z., & Miller, B. L. (2017). Epileptic activity in Alzheimer's disease: Causes and clinical relevance. *The Lancet Neurology*, *16*(4), 311–322. https://doi.org/10.1016/S1474-4422(17)30044-3

Washington, P. M., Morffy, N., Parsadanian, M., Zapple, D. N., & Burns, M. P. (2014). Experimental Traumatic Brain Injury Induces Rapid Aggregation and Oligomerization of Amyloid-Beta in an Alzheimer's Disease Mouse Model. *Journal of Neurotrauma*, *31*(1), 125–134. https://doi.org/10.1089/neu.2013.3017

Wei, C., Luo, Y., Peng, L., Huang, Z., & Pan, Y. (2021). Expression of Notch and Wnt/β-catenin signaling pathway in acute phase severe brain injury rats and the effect of exogenous thyroxine on those pathways. *European Journal of Trauma and Emergency Surgery*, *47*(6), 2001–2015. https://doi.org/10.1007/s00068-020-01359-4

Winer, J. R., Mander, B. A., Kumar, S., Reed, M., Baker, S. L., Jagust, W. J., & Walker, M. P. (2020). Sleep Disturbance Forecasts β-Amyloid Accumulation across Subsequent Years. *Current Biology*, *30*(21), 4291-4298.e3. https://doi.org/10.1016/j.cub.2020.08.017

Yan, P., Bero, A. W., Cirrito, J. R., Xiao, Q., Hu, X., Wang, Y., Gonzales, E., Holtzman, D. M., & Lee, J.-M. (2009). Characterizing the Appearance and Growth of Amyloid Plaques in APP/PS1 Mice. *The Journal of Neuroscience*, *29*(34), 10706–10714. https://doi.org/10.1523/JNEUROSCI.2637-09.2009

Zhang, F., Zhong, R., Li, S., Fu, Z., Wang, R., Wang, T., Huang, Z., & Le, W. (2019). Alteration in sleep architecture and electroencephalogram as an early sign of Alzheimer's disease

preceding the disease pathology and cognitive decline. *Alzheimer's & Dementia*, *15*(4), 590–597. https://doi.org/10.1016/j.jalz.2018.12.004